Plant Biotechnology Journal
Open Access

Plant Biotechnology Journal (2023) **21**, pp. 219–231 doi: 10.1111/pbi.13939

SPINDLY interacts with EIN2 to facilitate ethylene signalling-mediated fruit ripening in tomato

Jin Xu[1], Sidi Liu[1], Licong Cai[1], Lingyu Wang[1], Yufei Dong[1], Zhenyu Qi[2], Jingquan Yu[1,3] and Yanhong Zhou[1,3,4,*]

[1]*Department of Horticulture, Zijingang Campus, Zhejiang University, Hangzhou, China*
[2]*Agricultural Experiment Station, Zhejiang University, Hangzhou, China*
[3]*Key Laboratory of Horticultural Plants Growth and Development, Agricultural Ministry of China, Hangzhou, China*
[4]*Hainan Institute, Zhejiang University, Sanya, China*

Received 30 June 2022;
revised 26 September 2022;
accepted 28 September 2022.
**Correspondence* (Tel +86-571-88982276; fax +86-571-86971498; email yanhongzhou@zju.edu.cn)

Keywords: fruit ripening, ethylene signalling, *O*-glycosylation, SlSPY, SlEIN2.

Summary

The post-translational modification of proteins enables cells to respond promptly to dynamic stimuli by controlling protein functions. In higher plants, SPINDLY (SPY) and SECRET AGENT (SEC) are two prominent *O*-glycosylation enzymes that have both unique and overlapping roles; however, the effects of their *O*-glycosylation on fruit ripening and the underlying mechanisms remain largely unknown. Here we report that SlSPY affects tomato fruit ripening. Using *slspy* mutants and two *SlSPY*-OE lines, we provide biological evidence for the positive role of SlSPY in fruit ripening. We demonstrate that SlSPY regulates fruit ripening by changing the ethylene response in tomato. To further investigate the underlying mechanism, we identify a central regulator of ethylene signalling ETHYLENE INSENSITIVE 2 (EIN2) as a SlSPY interacting protein. SlSPY promotes the stability and nuclear accumulation of SlEIN2. Mass spectrometry analysis further identified that SlEIN2 has two potential sites Ser771 and Thr821 of *O*-glycans modifications. Further study shows that SlEIN2 is essential for SlSPY in regulating fruit ripening in tomatoes. Collectively, our findings reveal a novel regulatory function of SlSPY in fruit and provide novel insights into the role of the SlSPY-SlEIN2 module in tomato fruit ripening.

Introduction

Fruit ripening is a crucial developmental process mediated by a complex network of diverse factors including transcription factors, hormones and epigenetic switches (Giovannoni *et al.*, 2017). Physiological and molecular interventions have revealed that ethylene plays a prominent role in fruit ripening, especially in the case of climacteric fruits (Hamilton *et al.*, 1990; Oeller *et al.*, 1991). Ethylene is a versatile gaseous phytohormone that accumulates in response to various endogenous and exogenous stimuli and triggers a broad range of growth and developmental processes (Dong *et al.*, 2022; Johnson and Ecker, 1998). Extensive studies focused on ethylene biosynthesis and signalling in *Arabidopsis thaliana* have led to the characterization of a series of homologous genes in fruit-bearing species. The ethylene signalling pathway is activated when ethylene is perceived by the endoplasmic reticulum (ER)-localized receptors (Chang *et al.*, 2013). In *Arabidopsis*, the ER-localized membrane protein ETHYLENE INSENSITIVE 2 (EIN2) is a central regulator of ethylene signalling, which is evolutionarily conserved from green algae to land plants (Bisson *et al.*, 2009; Ju *et al.*, 2015). In the absence of ethylene, the negative regulator CONSTITUTIVE TRIPLE RESPONSE 1 (CTR1), a Raf-like Ser/Thr protein kinase, is activated by the hormone-free receptors (Kieber *et al.*, 1993) and inhibits ethylene signalling through phosphorylation of the C-terminal end of EIN2 (CEND) (Alonso *et al.*, 1999; Bisson and Groth, 2011). Meanwhile, the interaction of two F-box proteins, EIN2 TARGETING PROTEIN1 (ETP1) and EIN2 TARGETING PROTEIN2 (ETP2) with CEND results in the degradation of EIN2 by the ubiquitin-proteasome pathway (Qiao *et al.*, 2009). In contrast, inactivation of the receptors in response to ethylene results in lower CTR1 activity, which, in turn, triggers dephosphorylation of CEND and proteolytic cleavage leading to its ER-to-nucleus translocation (Ju *et al.*, 2012; Qiao *et al.*, 2012; Wen *et al.*, 2012). In the nucleus, the CEND transduces signals to the transcription factors ETHYLENE INSENSITIVE 3 (EIN3) and ETHYLENE INSENSITIVE 3-LIKE 1 (EIL1) with the subsequent transcriptional activation of a subset of ethylene response genes (Chao *et al.*, 1997; Zhang *et al.*, 2017).

Several types of post-translational modifications (PTMs) of proteins, such as methylation, acetylation, phosphorylation and ubiquitination are known for their roles in the regulation of fruit ripening. For example, the KDM5/JAR2DI sub-family of JmjC domain-containing proteins (SlJMJ6) encoding a ripening-prompting H3K27me3 demethylase activates the expression of genes associated with ripening by modulating H3K27me3 (Li *et al.*, 2020). In addition, histone deacetylases (HDACs) fine-tune the gene expression during ripening and in the kinetics of ripening (Tang *et al.*, 2020). Knockdown of *SlHDT3*, a tomato HDAC, results in delayed fruit ripening (Guo *et al.*, 2017). ETHYLENE RESPONSE 4 (SlETR4), a critical ethylene receptor, is repeatedly phosphorylated at different levels according to the ripening stage and ethylene action *in vivo* (Kamiyoshihara *et al.*, 2012). Based on the quantitative proteome analysis of nucleoproteins isolated from tomato fruits at various ripening stages, two specific E2 ubiquitin-conjugating enzymes, SlUBC32 and SlUBC41, have been proposed to be involved in fruit ripening (Wang *et al.*, 2014). Moreover, tomato *EIN3-BINDING F-BOX 3* (SlEBF3), encoding an E3 ubiquitin ligase mediates the degradation of SlEIL proteins (Deng *et al.*, 2018). Overexpression of *SlEBF3* results in reduced ethylene sensitivity and defective fruit ripening in tomato (Deng *et al.*, 2018). The past decade of research on glycan function has revealed that glycosyltransferases and glycosidases play an important role in the development and

physiological processes of living organisms (Ohtsubo and Marth, 2006). General *N*- and *O*-glycosylation systems that modify as many as half cellular proteins in eukaryotic organisms (Fletcher *et al*., 2009). Because of dozens of different *O*-glycan types, *O*-glycosylation is one of the most complex PTMs of proteins (Gao *et al*., 2021). Recently, an *O*-fucosyltransferase SPINDLY (SPY) was described in *Arabidopsis* where it modulates the function of DELLA by attaching monofucose to specific serine and threonine residues, which is opposed to the effect of nearby *O*-GlcNAcylation (Zentella *et al*., 2017). However, information about the role of *O*-glycosylation in fruit ripening remains elusive.

SPINDLY and SECRET AGENT (SEC) are two identified *O*-linked *N*-acetylglucosamine (O-GlcNAc) transferase (OGT) homologues in *Arabidopsis* (Hartweck *et al*., 2002). Among them, SEC has two homologous genes *SlSEC1* and *SlSEC2* in tomato. SPY and SEC were recently reported to have *O*-fucose and *O*-GlcNAc transferase activities, respectively, and antagonistically regulated DELLAs in gibberellin (GA) signalling (Zentella *et al*., 2017). In *Arabidopsis*, SPY and SEC have overlapping functions, which are necessary for gamete and seed development (Hartweck *et al*., 2006). To date, information about the role of SPY in phytohormone signalling is limited to GA-signalling and cytokinin response. SPY interacts with SWI3C, the core component of *Arabidopsis* SWI/SNF CRCs (Switch/Sucrose Non-fermenting-type chromatin-remodelling complexes) required for the proper functioning of DELLAs (Daviere and Achard, 2016; Sarnowska *et al*., 2013). SPY also interacts with two closely related class I TCP transcription factors to facilitate cytokinin responses in leaves and flowers (Steiner *et al*., 2012). However, the role of SPY-mediated *O*-glycosylation in other phytohormone responses is largely unknown. Therefore, studies on the role of SPY in other phytohormone signalling such as ethylene signalling in plant development, and the identification of the target protein modified by *O*-glycans are highly warranted.

In this study, we examine whether and how SPY is involved in ethylene-mediated fruit ripening in tomato. Strikingly, we found that *SlSPY* participates in tomato fruit ripening with its glycosyltransferase function. SlSPY-induced fruit ripening is linked to an increased response to ethylene. We show that SlSPY interacts with SlEIN2, thereby promoting fruit ripening. We also provide evidence that SlSPY promotes stability and nuclear accumulation of SlEIN2 protein. Taken together, our findings provide novel insights into the unique role of SlSPY in modulating fruit ripening and suggest that *O*-glycosylation plays a crucial role in the ethylene signalling pathway.

Results

SlSPY affects tomato fruit ripening

Firstly, we determined the changes in glucose, fructose and sucrose contents in tomatoes from 30 days post-anthesis (DPA) to 50 DPA. The results showed that the glucose and fructose contents roughly increased with the DPA but the sucrose content remained unchanged (Figure S1a). Intriguingly, glucose has been recognized to cause downstream *O*-glycosylation (Zachara and Hart, 2006). We then investigated the response of *O*-glycosylation in fruit ripening by analysing the transcripts of *O*-GlcNAc transferase homologues *SlSPY*, *SlSEC1* and *SlSEC2*. By constructing a phylogenetic tree of the SlSPY and SlSEC from tomato (*Solanum lycopersicum*), wild emmer wheat (*Triticum dicoccoides*), Arabidopsis (*Arabidopsis thaliana*), rice (*Oryza sativa*), field mustard (*Brassica rapa*) and human (*Homo sapiens*), based on the amino acid sequence alignments, we found that SlSPY and SlSEC belong to two groups (Figure S1b; Olszewski *et al*., 2010). qRT-PCR analysis showed that the transcripts of *SlSPY, SlSEC1* and *SlSEC2* all increased from 30 DPA and peaked at 45 DPA (Figure 1a). Importantly, *SlSPY* transcript abundance increases more than *SlSEC1* and *SlSEC2* (Figure 1a).

To investigate the role of SlSPY in fruit ripening, we generated 2 lines of *SlSPY* overexpressing plants *35Spro: SlSPY*-HA (*SlSPY#1* and *SlSPY#4*) and 2 lines of stable loss-of-function *slspy* mutants by CRISPR/Cas9-mediated gene editing (*slspy#1* and *slspy#2*). We selected 11-bp deletion mutations as *slspy#1* and 14-bp deletion mutations as *slspy#2* for further experiments. Both the 11-bp and 14-bp deletion mutations are predicted to cause premature stop codons in the exon coding Spy super family domain sequence. We did not find any off-target editing events in putative off-target sites (Figure S1c–e; Table S1). Fruits in the wild-type (WT) plants turned red at 45 DPA. This coloration was, however, accelerated in the *SlSPY* overexpressing plants and delayed in 2 lines of *slspy* mutants (Figure 1b). We then compared the accumulation of carotenoid content and fruit firmness in the WT, *slspy* and *35Spro: SlSPY*-HA fruits. The results showed that *SlSPY#1* and *SlSPY#4* fruits accumulated more carotenoids (lycopene, β-carotene, α-carotene, zeaxanthin and lutein) whilst *slspy#1* and *slspy#2* fruits accumulated less carotenoids compared to the WT fruits. Meanwhile, the *SlSPY#1* and *SlSPY#4* fruits had decreased firmness of pericarp whilst *slspy#1* and *slspy#2* fruits had increased firmness of pericarp (Figure 1c,d). In line with the accelerated onset of ripening, the transcript levels of several ripening-related genes, such as genes encoding phytoene synthase (*SlPSY1*), ζ-carotene desaturase (*SlZDS*), lipoxygenase (*SlLoxC*), polygalacturonase (*SlPG2a*), pectate lyases (*SlPL*) and ripening-related ethylene response factor *SlERF84*, were up-regulated in the *SlSPY#1* and *SlSPY#4* fruits and down-regulated in the *slspy#1* and *slspy#2* fruits compared with WT (Figure S2). These results indicate that the SlSPY is a positive regulator of fruit ripening in tomato.

SlSPY regulates fruit ripening by changing the ethylene response in tomato

Ethylene is the master phytohormone controlling the ripening of climacteric fruits. Strikingly, we found that ethylene production was unaffected in *slspy* and *35Spro: SlSPY*-HA fruits compared with WT fruits (Figure S3a,b). We thus examined the ethylene response of *slspy* and *35Spro: SlSPY*-HA lines to study whether *SlSPY*-induced fruit ripening was dependent on ethylene signalling. The fruits of *slspy*, WT and *35Spro: SlSPY*-HA at the mature green (MG) stage were treated with air, 1-methylcyclopropene (1-MCP, a competitive inhibitor of ethylene action) or ethylene. The results showed that the fruits of *slspy* plants had a lower accumulation of carotenoids after treatments with ethylene and air, compared with the WT fruits. In contrast, the accumulation of carotenoids in the fruits of *35Spro: SlSPY*-HA treated with ethylene was higher than those in the WT fruits (Figure 2a,b). Consistently, the *35Spro: SlSPY*-HA fruits showed decreased values in firmness but the *slspy* fruits showed increased values in firmness in response to both air and ethylene as compared to the WT fruits (Figure 2c). However, no significant difference in pericarp firmness was observed among the three genotypes upon 1-MCP treatment (Figure 2c). To further confirm the role of *SlSPY* in ethylene response, germinated seeds of *slspy* and *35Spro: SlSPY*-HA were exposed to ethylene precursor, 1-aminocyclopropane-1-carboxylic acid (ACC) (Figure 2d). In the

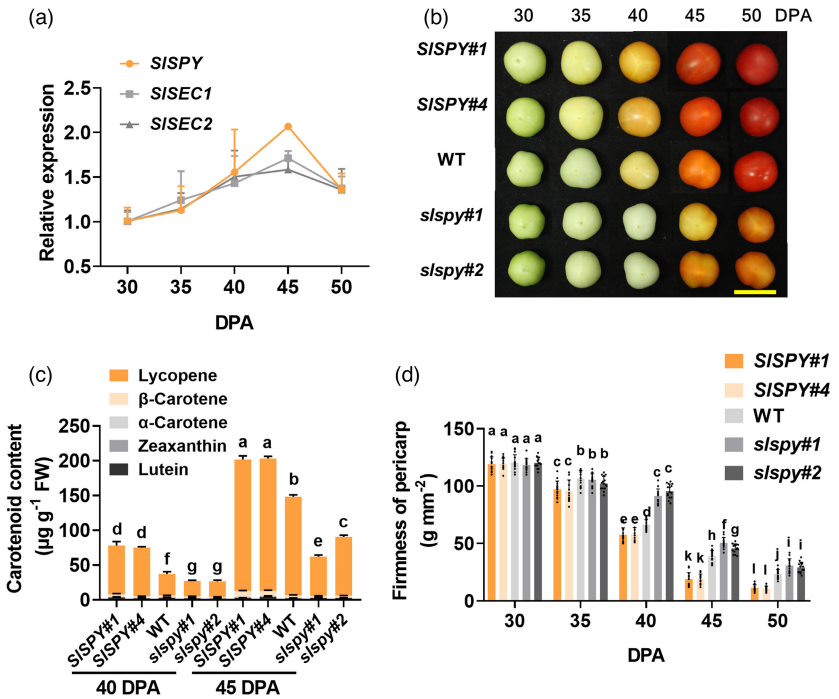

Figure 1 SlSPY affects tomato fruit ripening. (a) Relative transcript levels of *SlSPY, SlSEC1, SlSEC2* in tomato fruits at different ripening stages. Relative expression levels were normalized by the *Actin* expression level. The data are presented as mean values ± SD. $n = 3$ individual tomato fruits. (b) Phenotypes of fruit ripening in *slspy* mutants, *35Spro: SlSPY*-HA and WT plants. DPA, days post-anthesis. Scale bar, 2 cm. (c) Carotenoid content in fruits of *slspy* mutants, *35Spro: SlSPY*-HA and WT plants. Different letters indicate significant differences in total carotenoid content between samples ($P < 0.05$, Tukey's test). The data are presented as mean values ± SD. $n = 3$ individual tomato fruits. (d) Fruit firmness of *slspy* mutants, *35Spro: SlSPY*-HA and WT fruits at different ripening stages. Fifteen fruits were used for each measurement ($n = 15$), and the values shown are the means ± SD. Different letters indicate significant differences ($P < 0.05$) according to Tukey's test.

absence of ACC, the elongation of root and hypocotyl exhibited no significant difference among the *slspy*, WT and *35Spro: SlSPY*-HA seedlings. However, upon ACC treatment, the *slspy* seedlings showed decreased response to ACC with longer hypocotyls than the WT seedlings. In contrast, the *35Spro: SlSPY*-HA seedlings developed shorter hypocotyls and roots than the WT seedlings in the presence of ACC (Figure 2d–f). These results indicate that *SlSPY*-regulated fruit ripening is closely related to ethylene response in tomatoes.

SlSPY physically interacts with SlEIN2

To further explore the underlying mechanism by which SlSPY modulates ethylene-mediated fruit ripening, we investigated whether SlSPY interacts with the key components in the ethylene signalling pathway. Using a yeast two-hybrid (Y-2-H) screen with a library of tomato leaves, we identified SlEIN2 as a SlSPY interacting protein (Table S2). Y-2-H assay was then conducted to determine whether SlEIN2 could serve as a substrate of SlSPY. In the study, full-length SlEIN2 was replaced by a truncated SlEIN2C construct (SlEIN2C, encoding the C-terminal portion of SlEIN2 from amino acid residues 610–1316) as bait since full-length SlEIN2 as a transmembrane protein is not suitable for Y-2-H assay (Figure 3a). In *Arabidopsis*, the nuclear localization of C-terminal portion of EIN2 is required and sufficient for activating ethylene signalling (Wen *et al.*, 2012). We found that SlEIN2C indeed interacted with SlSPY in yeast cells (Figure 3b). The bimolecular fluorescence complementation assay (BiFC) was used to test whether this interaction occurs *in planta*. When co-transformed with SlSPY-cYFP (yellow fluorescent protein carboxy terminal) and SlEIN2C-nYFP (YFP amino terminal), fluorescence signals were observed in both cytoplasm and nucleus. In cells transformed with cYFP and SlEIN2C-nYFP or SlSPY-cYFP and nYFP, no fluorescence signal was detected (Figure 3c). Meanwhile, a co-immunoprecipitation (co-IP) assay was performed to further confirm the interaction of SlSPY and SlEIN2C *in vivo*. MYC-SlSPY was transiently co-expressed with SlEIN2C-HA or GUS-HA (as a negative control). After IP using anti-HA agarose conjugate, MYC-SlSPY was co-immunoprecipitated only when co-expressed with SlEIN2C-HA, but not with GUS-HA (Figure 3d), confirming the interaction between SlSPY and SlEIN2C *in planta*. Next, we expressed His-SlSPY and GST-tagged SlEIN2C (GST-SlEIN2C) recombinant fusion proteins in *Escherichia coli* and carried out a pull-down assay *in vitro*. The results showed that His-SlSPY interacted with GST-SlEIN2C, but not GST alone (Figure S4a). We also examined whether SEC-like *O*-GlcNAc transferase in tomato interacts with SlEIN2C by BiFC assays, and no fluorescence was detected in cells transformed with SlSEC1-cYFP and SlEIN2C-nYFP (Figure S4b). Furthermore, a very weak interaction between SlEIN2C and SlSEC1 was detected in yeast cells (Figure S4c). Taken together, multiple approaches were used to identify SlEIN2 as a SlSPY interacting protein.

To further investigate the exact domain mediating the interaction between SlSPY and SlEIN2, we conducted Y-2-H and co-IP assays with truncated proteins. It was found that the amino terminal contained the tetratricopeptide repeats (TPRs) domain (38–452 aa), rather than the carboxy terminal contained the Spy

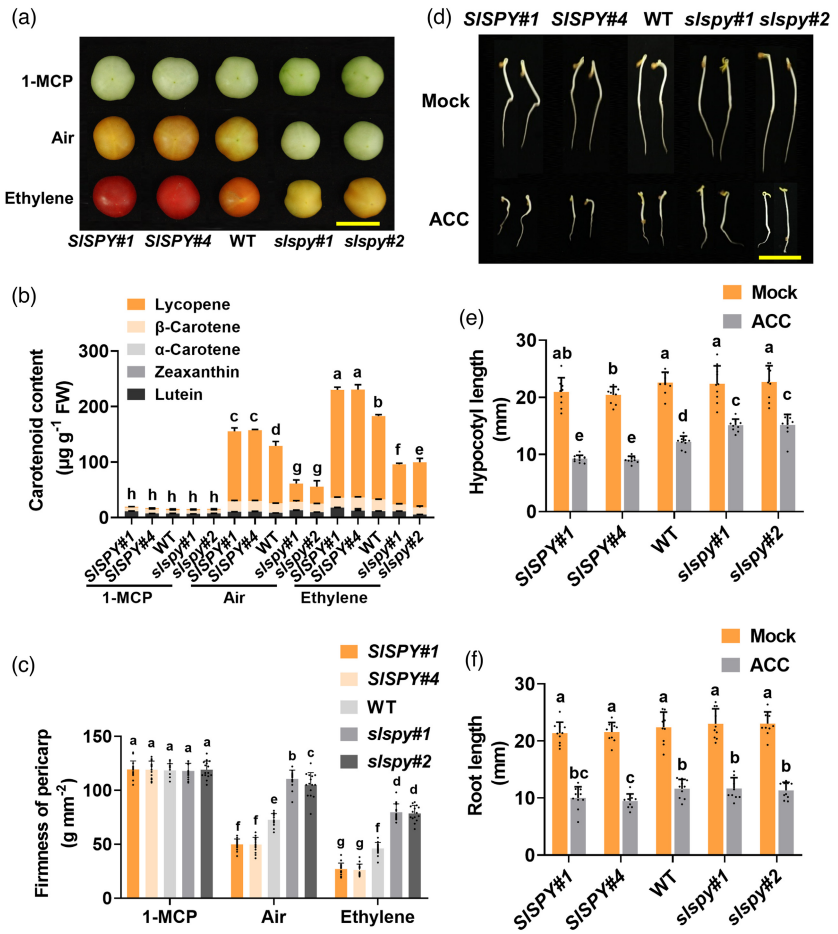

Figure 2 SlSPY regulates fruit ripening by changing the ethylene response in tomato. (a) Fruit phenotypes of *slspy* mutants, *35Spro: SlSPY*-HA and WT plants at 10 day after treatment with ethylene, air or 1-MCP, Scale bar, 2 cm. (b) Carotenoid content in *slspy* mutants, *35Spro: SlSPY*-HA and WT plants after 10 day with ethylene, air or 1-MCP treatment. Different letters indicate significant differences in total carotenoid content between treatments ($P < 0.05$, Tukey's test). The data are presented as mean values ± SD. $n = 3$ individual tomato fruits. (c) Fruit firmness of *slspy* mutants, *35Spro: SlSPY*-HA and WT plants after 10 days with ethylene, air or 1-MCP treatment. Fifteen fruits were used for each measurement ($n = 15$), and the values shown are the means ± SD. Different letters indicate significant differences ($P < 0.05$) according to Tukey's test. (d) Representative tomato seedling phenotypes of *slspy* mutants, *35Spro: SlSPY*-HA and WT plants after treatment with 20 μM ACC or not, Scale bar, 2 cm. (e) Hypocotyl lengths of tomato seedlings. The data are presented as mean values ± SD, $n = 10$ individual tomato seedlings. Different letters indicate significant differences ($P < 0.05$) according to Tukey's test. (f) Root lengths of tomato seedlings. The data are presented as mean values ± SD, $n = 10$ individual tomato seedlings. Different letters indicate significant differences ($P < 0.05$) according to Tukey's test.

superfamily domain (453–931 aa) predicted as the *O*-linked *N*-acetylglucosamine transferase, interacts with SlEIN2C in Y-2-H assay (Figure 3e,f). The results of Co-IP assay indicated that the SlEIN2C interacts with the SlSPY TPR domain but not the Spy superfamily domain (Figure 3g), further confirming that the interaction between SlEIN2 and SlSPY required the TPR domain of SlSPY. In addition, no fluorescence signal was detected in cells transformed with SlSPY-cYFP and SlEIN2N-nYFP (1–465 aa) when we performed BiFC assay (Figure S4d).

SlSPY regulates stability and nuclear accumulation of SlEIN2

Furthermore, to explore the biological function of SlSPY-SlEIN2 interaction, we then examined whether SlEIN2 can be *O*-glycosylated by SlSPY through co-expression of SlEIN2C-GFP with SlSPY-HA or GUS-HA in the mesophyll cells of *Nicotiana benthamiana* and higher-energy collisional dissociation (HCD)-mass spectrometry (MS) analysis was conducted. This allowed us to identify a peptide in the recombinant SlEIN2C-GFP purified from *N. benthamiana* mesophyll cells that had potential sites of *O*-GlcNAc modifications at Ser771 and Thr821 and *O*-fucose modifications at Ser771 (Figure 4a, Figure S5a,b). In contrast, we could not identify *O*-glycosylated peptides from SlEIN2C when SlEIN2C co-expressed GUS-HA.

We then investigated the biological significance of SlSPY-SlEIN2 physical interaction. Noticeably, SlEIN2C accumulated to higher levels after exposure to ACC for 6 h in *SlSPY#4* compared with WT (Figure 4b), indicating that SlSPY influences SlEIN2C protein accumulation. However, in tomato fruits at the Br stage, *SlEIN2* transcript levels did not change in the *slspy* and *35Spro: SlSPY*-HA plants compared with the WT plants, suggesting that the SlSPY-mediated change in SlEIN2 accumulation is not at the transcriptional level but at the post-transcriptional level (Figure S6). Hence, a cell-free degradation assay was then performed to examine whether SlEIN2C stability is affected by SlSPY. Immunoblotting analysis revealed a gradual degradation of the

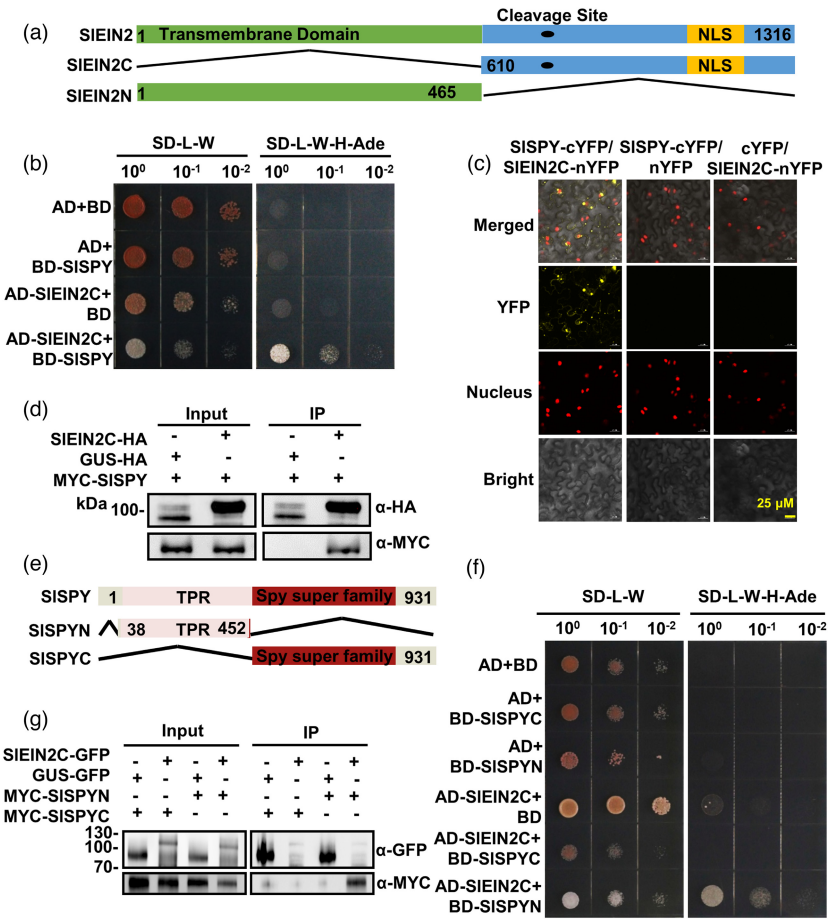

Figure 3 SlSPY physically interacts with SlEIN2. (a) Scheme for SlEIN2 fragments. The N-terminal fragment containing the transmembrane domain (SlEIN2N, 1–465 aa) and the C-terminal is required and sufficient for the activation of ethylene signalling (SlEIN2C, 610–1316 aa). NLS represents a distinct nuclear localization sequence. (b) Y-2-H assay of the interaction between SlSPY and C-terminal of SlEIN2C. The full-length coding sequence (CDS) of SlSPY was cloned into the bait vector pGBKT7. SlEIN2C was cloned into the prey vector pGADT7. AD vectors expressing AD-SlEIN2C were co-transformed with BD-SlSPY. SD-L-W, SD/-Leu/-Trp medium; SD-L-W-H-Ade, SD/-Leu/-Trp/-His/-Ade. (c) In BiFC assays, SlSPY interacts with SlEIN2C *in vivo*. *N. benthamiana* was co-transformed with SlSPY-cYFP and SlEIN2C-nYFP, SlSPY-cYFP and nYFP or cYFP and SlEIN2C-nYFP. H3-mCherry as a red fluorescence signal located at the nucleus. Scale bars, 25 μM. (d) Interactions between MYC-SlSPY and SlEIN2C-HA measured by co-IP assays. Total protein extracts (Input) and protein complexes immunoprecipitated with anti-HA agarose (IP) were detected by anti-HA and anti-MYC antibodies. (e) Scheme for SlSPY fragments. The N-terminal fragment containing the TPR domain (SlSPYN, 38–452aa) and the C-terminal containing the Spy super family domain (SlSPYC, 453–931 aa). (f) Y-2-H assay of the interaction between SlSPYC, SlSPYN and SlEIN2C. The truncated fragment SlSPYC and SlSPYN were cloned into the bait vector pGBKT7. SlEIN2C was cloned into the prey vector pGADT7. AD vectors expressing SlEIN2C were co-transformed with BD-SlSPYC and BD-SlSPYN. (g) Interactions between MYC-SlSPYC, MYC-SlSPYN and SlEIN2C-GFP measured by co-IP assays. Total protein extracts (Input) and protein complexes immunoprecipitated with anti-GFP agarose (IP) were detected by anti-GFP and anti-MYC antibodies.

purified recombinant His-SlEIN2C, and MG132 (an inhibitor of 26S proteasome-mediated proteolysis) treatment apparently reduced its degradation, indicating that SlEIN2 degradation is partial dependent on the 26S proteasome pathway. We prepared extracts from WT and *SlSPY#4*, respectively, to test His-SlEIN2C degradation in cell-free extracts. Consistent with the previous studies, the degradation of His-SlEIN2C was delayed in *SlSPY#4* extracts (Figure 4c). Next, we tested SlEIN2C stability by western blotting after treatment with cycloheximide (CHX), which inhibits *de novo* protein biosynthesis. A slower loss of SlEIN2C-GFP was observed in the *N. benthamiana* cells compared to SlEIN2C$^{S771A/T821A}$-GFP. Both SlEIN2C-GFP and SlEIN2C$^{S771A/T821A}$-GFP levels dramatically decreased after 1 h of CHX treatment and remained barely detectable for 2 h (Figure 4d). Taken together, these results indicate that SlSPY stabilizes SlEIN2C and prevents its proteolysis.

The BiFC assays were then conducted to explore the interaction between SlEIN2 and SlSPY and its subcellular localization. We found that SlEIN2 and SlSPY show different subcellular localization when they exist alone; that is, SlEIN2 is localized in the ER membrane as known while SlSPY is a nucleocytoplasmic shuffling protein (Maymon *et al.*, 2009; Swain *et al.*, 2002) (Figure S7a). However, it was found that SlEIN2 interacts with SlSPY in the cytoplasmic foci (Figure 4e; Figure S7b; Movie S1). To investigate whether the nuclear accumulation of SlEIN2 protein was affected by SlSPY, we separated tomato protein extracts into cytosolic and nuclear fractions. The SlEIN2C protein levels were increased in total protein extracts from *SlSPY#4* compared to the WT. Importantly, the nuclear abundance of SlEIN2C was much higher in *SlSPY#4* relative to the WT (Figure 4f). To further examine the accumulation of SlEIN2C in the nuclei affected by *O*-glycosylation,

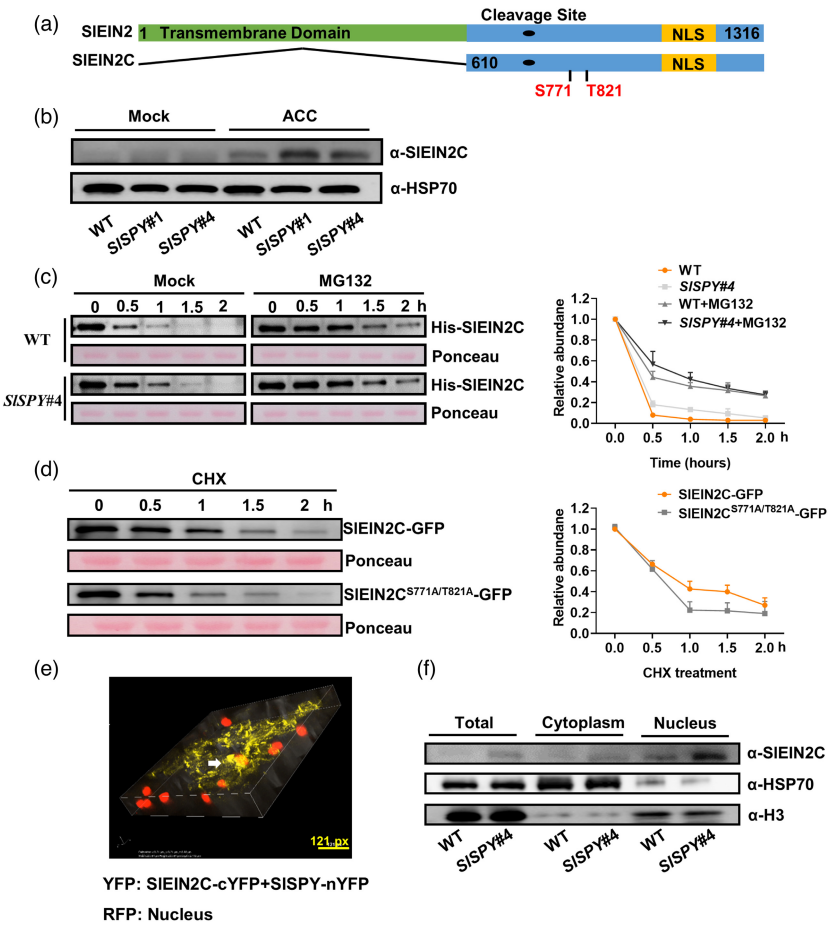

Figure 4 SlSPY regulates stability and nuclear accumulation of SlEIN2. (a) Scheme for SlEIN2 fragments. The red label indicates the position of the *O*-glycans modification sites. (b) Accumulation of SlEIN2C protein in WT and *SlSPY#4* after exposure to ACC for 6 h or not. SlEIN2C protein abundance was detected with an anti-SlEIN2C antibody. HSP70 was used as a lane loading control. (c) 100 ng of recombinant His-SlEIN2C protein was incubated in 100 μL extracts for the individual assay. *SlSPY#4* delayed His-SlEIN2C degradation in the cell-free system. Protein extracts were extracted from 4-week old WT or *SlSPY#4* tomato seedlings and then incubated with or without 50 μM MG132 over the indicated time course. Ponceau staining as a lane loading control. (d) Transient expression of SlEIN2C-GFP and SlEIN2C$^{S771A/T821A}$-GFP in *N. benthamiana* leaves treated with 10 mM CHX for different amounts of time. Total protein lysates were subjected to immunoblotting with anti-GFP. Ponceau staining as a lane loading control. (e) A 3D image showing that SlEIN2 interacts with SlSPY is present in cytoplasmic foci. The white arrow indicates the overlapping part between YFP and RFP. H3-mCherry is a red fluorescence signal located at the nucleus. (f) Immunoblot assay showing the accumulation of SlEIN2C in WT and *SlSPY#4*. The abundance of SlEIN2C was detected with an anti-SlEIN2C antibody. HSP70 and Histone H3 were used respectively as cytoplasm and nucleus loading control.

a construct carrying a base substitution in SlEIN2C that converts serine/threonine (S/T) to alanine (A) (S771A/T821A) was expressed in *N. benthamiana* leaves. Much stronger green fluorescence signals were detected in the nuclei of cells transformed with SlEIN2C-GFP than SlEIN2C$^{S771A/T821A}$-GFP, in which green fluorescence signals co-localized with H3-mCherry (red fluorescence signals located in the nucleus), while deletion of the nuclear localization sequence (NLS) retained the SlEIN2C-GFP fusion protein exclusively in the cytoplasm (Figure S7c,d). Collectively, these results suggest that SlSPY promotes the nuclear accumulation of SlEIN2.

SlEIN2 is required for the function of SlSPY in fruit ripening

Given that SlEIN2 is subjected to the regulation by SlSPY, therefore, *SlEIN2* in the fruits of WT and *SlSPY#4* were silenced using virus-induced gene silencing (VIGS) (Figure S8a). In contrast to the accelerated fruit ripening in the *SlSPY* overexpressed plants, silencing *SlEIN2* delayed the ripening of the fruits, compared with the WT fruits. Importantly, overexpression of *SlSPY* failed to restore the ripening of pTRV-*SlEIN2* (*SlEIN2*-silenced plants; Figure 5a–c). Finally, both pTRV-*SlEIN2* and *SlSPY#4*: pTRV-*SlEIN2* showed a lower carotenoid content and a higher fruit firmness than WT: pTRV and *SlSPY#4*: pTRV at 45 DPA (Figure 5a–c). These results indicate that SlEIN2 is required for the function of SlSPY in fruit ripening.

SlSPY is involved in ethylene signalling

Experiments were then performed to determine the role of SlSPY in the regulation of ethylene signalling. Immunoblot analysis using anti-SlEILs antiserum revealed that SlEILs protein accumulation markedly decreased in *slspy* lines (Figure 6a). The transcript levels of ripening-related genes, such as *SlPSY1*, *SlZDS*, *SlLoxC*, *SlPG2a*, *SlPL* and ripening-related ethylene response factor

SlERF84, were up-regulated in the WT and *SlSPY#4* fruits, but silencing *SlEIN2* prevented the up-regulation of these genes at 45 DPA (Figure 6b). During vegetative growth, *slspy* mutants displayed slightly dwarf phenotype compared with WT (Figure S9a). In line with the phenotype of loss-of-function *slein2-1* mutant (Huang *et al*., 2022), *slspy#1* had smaller fruit size as well as decreased seed number (Figure S9b). Moreover, leaf and petal senescence were delayed in the *slspy#1* mutant (Figure S9c,d). In addition, both WT and *slspy* mutants were exposed to mechanical stress and salt stress to verify the role of SlSPY in ethylene response. Mechanical stress induced a significant increase in the abundance of *SlERF7* and *SlERF52* transcripts only in WT plants, but not in *slspy* lines (Figure S8b). Consistent with this, an accumulation of *SlERF9* and *SlERF30* transcripts after salt stress was only observed in WT plants, but not in *slspy* lines (Figure S8c).

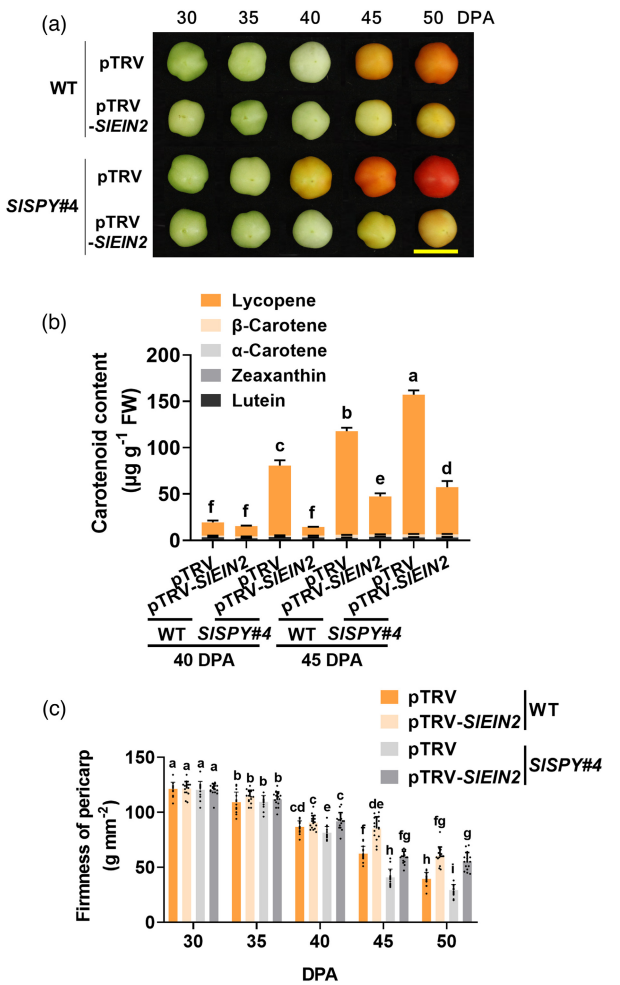

Figure 5 SlEIN2 is required for the function of SlSPY in fruit ripening. (a) Fruit phenotypes from WT, *SlSPY#4*, pTRV-*SlEIN2* and *SlSPY#4* pTRV-*SlEIN2* at different ripening stages. Scale bar, 2 cm. (b) Carotenoid content of WT, *SlSPY#4*, pTRV-*SlEIN2* and *SlSPY#4* pTRV-*SlEIN2* at different ripening stages. Different letters indicate significant differences in total carotenoid content between samples ($P < 0.05$, Tukey's test). The data are presented as mean values ± SD. $n = 3$ individual tomato fruits. (c) Fruit firmness of WT, *SlSPY#4*, pTRV-*SlEIN2* and *SlSPY#4* pTRV-*SlEIN2* fruits at different ripening stages. Fifteen fruits were used for each measurement ($n = 15$), and the values shown are the means ± SD. Different letters indicate significant differences ($P < 0.05$) according to Tukey's test.

Taken together, our results suggest that SlSPY is involved in ethylene signalling.

Discussion

Ethylene has profound effects on fruit ripening in climacteric fruits, and its production is closely associated with the ripening phenotypes such as carotenoid accumulation, softening, accumulation of soluble solids and emission of aroma volatiles (Oeller *et al*., 1991). One critical challenge to understanding the molecular basis for the fruit maturation process is to elucidate the transduction process of ethylene signalling during fruit ripening. In this study, we demonstrate that SlSPY-dependent *O*-glycosylation of SlEIN2 plays a critical role in fruit ripening in tomato. SlSPY directly interacts with SlEIN2 to promote the *O*-glycans modification status of SlEIN2. This modification of SlEIN2 affects its stability and nuclear accumulation in order to fine-tune ethylene-promoted fruit ripening in tomato (Figure 7).

The role of glucose in mediating cellular processes has become increasingly clear over the past several years. One downstream effector produced from glucose is UDP-GlcNAc (Zachara and Hart, 2006). Protein *O*-GlcNAcylation is known to play an important role in developmental regulation, stem cell maintenance, circadian regulation and responses to external light and temperature stimuli (Steiner *et al*., 2012; Xiao *et al*., 2014; Xing *et al*., 2018; Zentella *et al*., 2016). Recently, it has been recognized that nucleocytoplasmic *O*-GlcNAc is replaced by *O*-fucose in many protists (West and Kim, 2019). A similar *O*-fucosyltransferase was recently described in *Arabidopsis* where it modulates the function of a nuclear transcriptional regulator DELLA protein RGA by attaching monofucose to specific serine and threonine residues (Zentella *et al*., 2017). Here, we found that fruit ripening is accompanied by an increased accumulation of glucose, *SlSPY* and *SlSEC* transcripts (Figure S1a; Figure 1a). Importantly, overexpression of *SlSPY* accelerated fruit ripening and increased the total carotenoid content compared to the WT fruits, while mutation of *SlSPY* delayed fruit ripening and decreased the total carotenoid content (Figure 1b,c). Meanwhile, SlSPY regulates fruit ripening by changing the ethylene response in tomato (Figure 2). To our knowledge, this is the first report on the role of SPY in fruit development.

SlSPY as a glycosyltransferase plays a pivotal role in fruit ripening by increasing ethylene responses in tomato (Figures 1 and 2). In agreement with this, earlier studies showed that SPY participates in the regulation of the GA pathway by *O*-glycosylating the GA-signalling protein DELLAs in *Arabidopsis* (Zentella *et al*., 2017), while SPY positively mediates cytokinin responses to control leaf serration phenotype (Greenboim-Wainberg *et al*., 2005). Here, we found that SlSPY interacted with SlEIN2 through the SlSPY TPR domain and SlEIN2 C-terminus *in vitro* and *in vivo* (Figure 3b–f). It has been shown that SPY plays a role in protein *O*-fucosylation (Wang *et al*., 2020; Zentella *et al*., 2017). MS analysis indicated that SlEIN2 served as a substrate of SlSPY and can be *O*-glycosylated (Figure S5a,b). Both *O*-GlcNAcylated and *O*-fucosylated SlEIN2 peptides were detected when co-expressed with SlSPY-HA (Figure S5a,b). Meanwhile, SEC is another OGT having related functions for embryogenesis as the *sec spy* mutant is embryo-lethal in *Arabidopsis* (Hartweck *et al*., 2002). Although the transcripts of *SlSEC1* and *SlSEC2* increased during the fruit ripening, both the BiFC assay and Y-2-H assay failed to detect physical interaction between SlSEC1 and SlEIN2C (Figure S4b,c), suggesting that

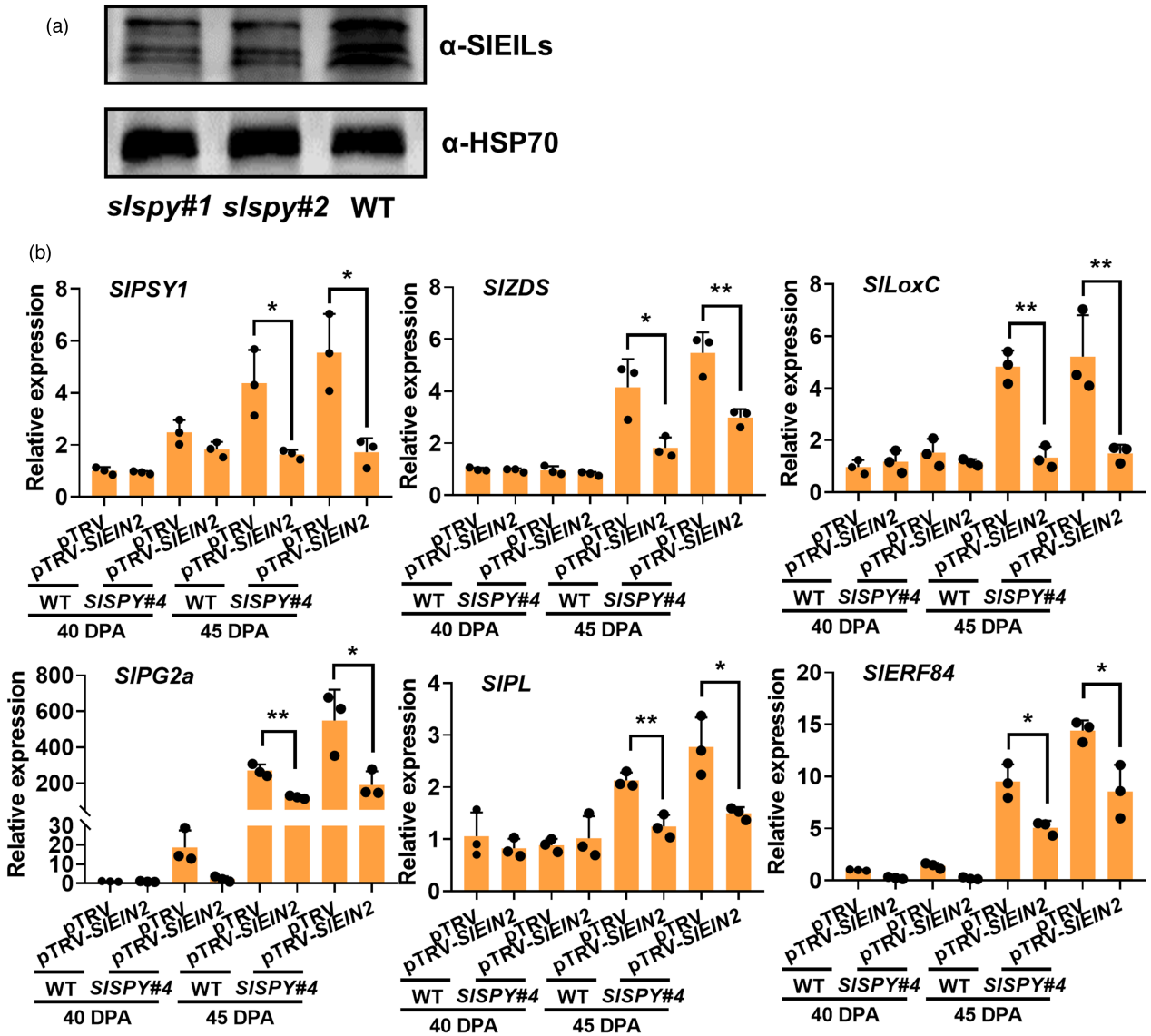

Figure 6 Relative expression of ripening-related genes in WT, *SlSPY#4*, pTRV-*SlEIN2* and *SlSPY#4* pTRV-*SlEIN2* at different ripening stages. (a) Immunoblot analysis using anti-SlEILs antibody in WT and *slspy* lines. HSP70 was used as a loading control. (b) Relative transcript levels of ripening-related genes in WT, *SlSPY#4*, pTRV-*SlEIN2* and *SlSPY#4* pTRV-*SlEIN2* fruits were determined by qRT-PCR. Relative expression levels were normalized by the *Actin* expression level. The relative expression level of WT fruit was assigned a value of 1. Data are the means ± SD. $*P < 0.05$, $**P < 0.01$ (Student's *t*-test). At least three independent experiments were performed.

SlEIN2 is more likely targeted by SlSPY rather than by SlSEC. It remains to be studied whether SPY participates in fruit ripening through *O*-GlcNAcylation or *O*-fucosylation. Taken together, our study demonstrates that SlSPY plays a role in fruit ripening by modifying the central ethylene signalling component SlEIN2.

EIN2 is a protein with a short half-life and proteasome-mediated EIN2 turnover is essential for triggering appropriate ethylene responses in plants (Qiao *et al.*, 2009). According to previous research, the nuclear localization of CEND is required and sufficient for activating ethylene signalling (Wen *et al.*, 2012). After exposure to ACC, SlEIN2C accumulated to higher levels in *SlSPY#4* compared with WT (Figure 4b). We found that SlSPY plays a role in the stabilization of SlEIN2 and prevents its proteolysis (Figure 4b–d). EIN2 undergoes rapid proteasome-mediated turnover because of being targeted by ETP1/ETP2 F-box proteins (Qiao *et al.*, 2009). It is thus possible that *O*-glycosylation participates in EIN2 proteasome-mediated turnover. Thereafter, it is important to determine whether *O*-glycosylation alters the targeting of EIN2 to the proteasome or the activity of the proteasome.

The EIN2 C-terminal is located both in the cytoplasm and nucleus, and it guarantees the stabilization of key transcription factors EIN3/EIL1 in response to ethylene accumulation (Li *et al.*, 2015; Merchante *et al.*, 2015; Qiao *et al.*, 2012). Early studies showed that nuclei and the soluble fraction of rat liver cells are particularly rich in proteins bearing *O*-linked GlcNAc residues (Holt and Hart, 1986). Consistent with that, a rapidly shuttling from the cytoplasm to the nucleus was observed in several *O*-GlcNAc modified proteins in *Aplysia* neurons (Elliot *et al.*, 1993), indicating that *O*-GlcNAc may be an alternative NLS

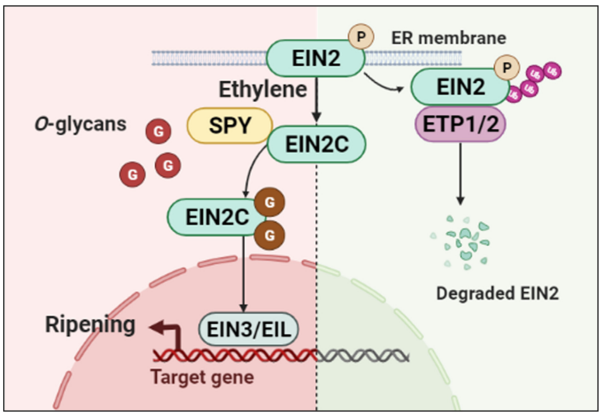

Figure 7 Working model for SlSPY interacting with SlEIN2C to facilitate ethylene responses in tomato fruits. In response to ethylene, SlSPY directly interacts with SlEIN2C to promote the *O*-glycans modification status of SlEIN2C (left). EIN2 contributes to the stabilization of EIN3/EILs, which are necessary for the transcriptional activation of ethylene response genes. Our work shows that SlSPY acts by regulating the ethylene signalling pathway to acquire ripening-promotive ethylene responsiveness.

signal or nuclear retention signal. In the present study, the mutation of potential sites of *O*-glycans modification in SlEIN2 leads to a decrease in the nuclear accumulation of SlEIN2 (Figure 4f, Figure S7c and d). Therefore, *O*-glycosylation of SlEIN2 regulates the nuclear accumulation of SlEIN2 C-terminal, which is shuttling between the cytoplasm and nucleus and modulates ethylene signal transduction. The molecular mechanism by which SlEIN2 achieves this shuttling responded to ethylene and whether *O*-glycosylation of SlEIN2 affects SlEIN2 nuclear localization remains unclear.

Recent studies show that there is extensive crosstalk between *O*-GlcNAcylation and phosphorylation (Hart *et al.*, 2011). Many proteins are reciprocally modified under different conditions at the same site or at proximal sites by either *O*-GlcNAc or phosphate (Hart *et al.*, 2011). Multiple post-translational modifications are at either shared or distinct sites giving the cell greatly expanded molecular diversity. In fact, EIN2 contains predicted sites for both phosphorylation and *O*-GlcNAcylation (Xu *et al.*, 2017). It has been previously reported that ethylene triggers dephosphorylation at several sites at EIN2 leading to ER-to-nucleus translocation of CEND and improved EIN2 protein stability (Qiao *et al.*, 2009; Qiao *et al.*, 2012). Therefore, it is likely that *O*-glycosylation of SlEIN2 improves its protein stability and regulates CEND shuttling between the cytoplasm and nucleus by maintaining dephosphorylation status. The exact relationship between *O*-glycosylation and phosphorylation of SlEIN2 needs to be further determined.

In *Arabidopsis*, EIN2 is required for all ethylene responses and constitutes a critical part in the ethylene signal transduction pathway. It acts between CTR1 and the EIN3/EIL transcription factors and contributes to the stabilization of EIN3/EILs in ethylene signalling (Liu *et al.*, 2015). As compared with *Arabidopsis*, tomato and other fruit species have distinct expression patterns and often expanded families of genes encoding ethylene signalling components, but the pathway activities are well conserved among species (Giovannoni *et al.*, 2017). In agreement with this, overexpression of *SlSPY* failed to restore the ripening of *SlEIN2*-suppressed fruits (Figure 5a–c). Immunoblot analysis revealed that SlEILs protein accumulation markedly decreased in *slspy* lines (Figure 6a). The transcripts of several ripening-related genes increased in the WT and *SlSPY#4* fruits, but silencing *SlEIN2* prevents these genes from up-regulated at 45 DPA (Figure 6b). Furthermore, SlSPY is linked to the transcripts of many ethylene-related genes in response to abiotic stress as mechanical or salt stress-induced transcripts of *SlERF7, SlERF52*, *SlERF9* and *SlERF30* were notably repressed in *slspy* lines (Figure S8b,c). Given that ethylene participates in the regulation of many stress responses such as mechanical, salt and oxidative stresses, it will be interesting to study the role of SPY-dependent *O*-glycosylation of EIN2 in the response to these stresses.

Materials and methods

Plant materials and growth conditions

The wild-type tomato (*S. lycopersicum* L. cv. Micro-Tom) and transgenic lines in this background (two CRISPR-Cas 9 mutant lines *slspy#1* and *slspy#2* and two OE lines *SlSPY#1* and *SlSPY#4*) were grown in growth chambers with a 12 h photoperiod at 25 °C/20 °C (day/night) temperature and 600 μmol/m^2/s photosynthetic photon flux density. In addition, *Nicotiana benthamiana* for transient expression were grown in growth chambers with 16-h light/8-h dark cycles at 25 °C/20 °C (day/night) temperature.

Constructs and plant transformation

To generate mutant lines, sgRNA oligo were designed containing 20-bp targeting the exon of SlSPY (5′-TGTAGTTC ATGGCAAGTAAC-3′; Mao *et al.*, 2013), which was annealed and inserted into AtU6-sgRNA-AtUBQ-Cas9 vector. The cassette was then subcloned into the pCambia1301 binary vector, which were transformed into tomato cv. Micro-Tom by *Agrobacterium tumefaciens*-mediated cotyledon tissue culture. All transgenic plants were genotyped by PCR of genomic DNA flanking the target site (Table S3). To obtain the tomato *SlSPY* overexpressing construct, the 2793-bp full-length coding DNA sequence was cloned into plant transformation vector pFGC1008-HA (Table S4) behind the CaMV 35S promoter. Two independent homozygous lines of the T2 generation were used for the study.

Virus-induced gene silencing (VIGS) in tomato fruits

A 300-bp fragment of the *SlEIN2* gene corresponding to bases 3151–3450 of the *SlEIN2* gene was PCR-amplified from tomato cDNA (Table S4) and then subcloned into pTRV2 to generate pTRV2-*SlEIN2*. The resulting confirmed plasmids were introduced into *Agrobacterium tumefaciens* strain GV3101. Virus-induced gene silencing in tomato fruits was conducted as previously described (Fantini and Giuliano, 2016; Fu *et al.*, 2005). Silencing efficiency was identified by quantitative real-time PCR (qRT-PCR) using the specific primers (Table S5).

Chemical treatment

For studying the ethylene response of transgenic tomato, tomato fruits at the MG stage were placed into an air-tight 500 mL plastic container with 500 μL/L ethylene solution (Xu *et al.*, 2012) or 10 μL/L 1-methyl cyclopropene (1-MCP; 48 mg of 1-MCP-releasing powder dissolved in 50 μL of water) (Fujisawa *et al.*, 2013). The fruits were treated for 24 h and then transferred to open air for 10 day. As the control, an equal volume of double distilled water was used as a negative control

instead of ethylene or 1-MCP. After the treatment, fruit pericarp was sampled for carotenoid content analysis. For ethylene response assay of tomato seedlings, 20 μM ACC (Sigma-Aldrich) was selectively added to 1/2 MS medium incubating tomato germinated seeds. For cycloheximide (CHX) treatment, 5 mM CHX was injected into *N. benthamiana* leaves.

RNA extraction and qRT-PCR analysis

Total RNA was extracted using a Plant RNA Purification Reagent (Invitrogen, cat. no. 12322-012). DNA depletion (Promega) and reverse transcription (ReverTra Ace quantitative qPCR RT kit, Toyobo) were performed according to the manufacturer's instructions. qRT-PCR was performed using SYBR Green PCR Master Mix (Vazyme) with the LightCycler 480 real-time PCR system (Roche Diagnostics). Primers are listed in Table S5.

Measurement of the soluble sugar content

Three grams of tomato fruit powder were poured into a 50 mL centrifuge tube filled with 10 mL of 80% absolute ethanol. The centrifuge tube was placed in an 80 °C water bath for 60 min, the extracts were mixed well and centrifuged at 10 000 ***g*** for 10 min at 4 °C, distilled water was added to bring the volume to 25 mL and soluble sugar extract was measured by high-performance liquid chromatography (HPLC; Xia *et al*., 2021).

Measurement of carotenoid content, firmness and ethylene production of fruit

Carotenoid extraction was performed as described previously (Fantini *et al*., 2013). Briefly, tomato fruit powder was extracted with 700 μL chloroform, 350 μL ddH_2O and 350 μL methanol. The extracts were mixed well and centrifuged at 10 000 ***g*** for 10 min at 4 °C, and the chloroform phase was collected. Afterward, 700 μL chloroform was added to the remaining residue, and the above steps were repeated until the chloroform phase became colourless. The combined organic phases were then dried by blowing nitrogen gas and resuspended in 350 mL of methanol including 6% KOH (w/v) for 30 min at 60 °C. After adding 700 μL chloroform and 350 μL ddH_2O, the solution was mixed well and centrifuged at 10 000 ***g*** for 10 min at 4 °C, and the chloroform phase was collected. Then 700 μL chloroform was added to the remaining residue, the above steps were repeated until the chloroform phase was colourless. The combined organic phases were then dried by nitrogen blowing and resuspended in 100 μL of ethyl acetate and injected for ultra-performance liquid chromatography analysis (Thermo Fischer Scientific). The firmness of the pericarp was assayed using TA. XTplus Texture Analyser (Stable Micro Systems, UK) according to the manufacturer's instructions. For the measurement of ethylene production in fruits, each fruit was placed in a 110 mL gastight container at 25 °C for 1 h, and 1 mL of headspace gas sample was analysed with gas chromatography (Agilent Technologies 7890A GC System).

Protein extraction and immunoblot analyses

Fruit proteins were isolated according to the protocol as previously described (Rocco *et al*., 2006). Protein concentration was quantified by Bradford assay. Nuclear proteins were extracted from tomato seedlings as previously described (Sikorskaite *et al*., 2013).

Immunoblot analysis was performed using specific antibodies, including, anti-GFP antibody (Immunoway), anti-H3 antibody (Agrisera), anti-HA antibody (Thermo Fisher), anti-MYC antibody (Millipore), anti-GST antibody (Cell Signalling Technology), anti-His antibody (Cell Signalling Technology), anti-HSP70 antibody (Agrisera), anti-SlEILs antibody, anti-SlEIN2C antibody.

Pull-down assays

C-terminal of SlEIN2 (SlEIN2C, 610–1316 aa) was cloned into pGEX-4T-1 to generate GST-SlEIN2C, and *SlSPY* was cloned into pET-32a to generate His-SlSPY (Table S6). These proteins were expressed and purified from *E. coli* Rosetta. The pull-down analyses were performed as reported (Miernyk and Thelen, 2008). Anti-GST agarose beads were used to pull-down the protein complexes. The protein blots were analysed using an anti-His antibody.

Yeast two-hybrid (Y-2-H) assays

The coding sequences of *SlSPY*, *SlSEC*, *SlEIN2C*, *SlSPYC* and *SlSPYN* were amplified (Table S7). *SlEIN2C* was inserted into the pGADT7 vector (Clonetech), and *SlSPY*, *SlSEC*, *SlSPYC* and *SlSPYN* were inserted into the pGBKT7 vector (Clonetech), respectively. Y-2-H assays were performed following the manufacturer's instructions.

Co-immunoprecipitation (co-IP) assays

The CDS of *SlSPY*, *SlSPYC* and *SlSPYN* without stop codon was fused with 6 × MYC tags and then cloned into pCambia1301 vector, SlEIN2C and GUS without stop codon was fused with 3 × HA tags or GFP (Table S4). Recombinant vectors were transfected into *A. tumefaciens* strain GV3101 separately as described in Waadt and Kudla (2008). After 48 h, *N. benthamiana* leaves were harvested. The protein extracts were incubated with anti-HA agarose (Sigma-Aldrich) or anti-GFP agarose (Clontech) for 1 h. After eluting the retained proteins on beads using the Laemmli loading buffer at 65 °C for 10 min, the protein blots were analysed using an anti-MYC antibody.

Bimolecular fluorescence complementation (BiFC) assays

Recombinant vectors SlSPY-cYFP, SlSEC-cYFP, SlEIN2C-nYFP were transfected into GV3101 separately (Table S4), transient expression were performed (Sparkes *et al*., 2006). The BiFC assay procedures were previously described (Waadt and Kudla, 2008). A laser confocal scanning microscope (ZEISS Microsystems LSM 700) were used to observe the infiltrated leaves. H2B-mCherry was used as a nuclear marker.

Subcellular localization

Recombinant vectors SlSPY-GFP, SlEIN2C-GFP, $SlEIN2C^{S771A/T821A}$-GFP and SlEIN2CΔNLS-GFP were transfected into GV3101 separately (Table S4), transient expression were performed (Sparkes *et al*., 2006). The assay procedures were described previously (Waadt and Kudla, 2008). A laser confocal scanning microscope (ZEISS Microsystems LSM 700) were used to observe the infiltrated leaves.

Cell-free degradation assay

The leaves of tomato seedlings were ground in liquid nitrogen to form fine powders. The total proteins were then extracted using a degradation buffer and the degradation assay was performed as previously described (Wang *et al*., 2009). Each individual assay used 100 ng of recombinant His-SlEIN2C protein incubated in 100 μL total proteins extracts. The protein blots were analysed using an anti-His antibody.

Mass spectrometry analysis of SlEIN2

Recombinant SlEIN2C-GFP purified from *N. benthamiana* mesophyll cells. LC–MS/MS analysis was performed by Shanghai Applied Protein Technology. DTT and iodoacetamide were used to reduce and block the cysteine residues. A 20-h incubation with trypsin followed. Each fraction was injected for nano-LC–MS/MS analysis.

Abiotic stress response assays

For mechanical stress, the fourth leaves of the 6-leaf stage plants were squeezed twice with forceps. For salt stress, plants at the 6-leaf stage were grown in Hoagland's complete nutrient solution with or without 200 mM NaCl for 4 h. Leaf tissue samples were harvested and frozen in liquid nitrogen immediately. Untreated seedlings were used as control.

Statistical analysis

Unless otherwise specified, each experiment contained 12–15 plants, and at least three biological replicates were used. One-way ANOVA was used to analyse the data using SPSS20. No statistically significant differences were found in the means between the shared letters ($P > 0.05$). Relative transcript levels of ripening-related genes in WT, *SlSPY#4*, pTRV-*SlEIN2* and *SlSPY#4* pTRV-*SlEIN2* and relative transcript levels of *SlERF7*, *SlERF52*, *SlERF9* and *SlERF30* were statistically analysed using Student's *t*-test.

Acknowledgements

We are grateful to the Tomato Genetics Resource Center (TGRC) for tomato seeds. We also thank Xiaodan Wu and Nan Wang (Analysis Center of Agrobiology and Environmental Sciences, Institute of Agrobiology and Environmental Sciences, Zhejiang University) for assistance with carotenoid and soluble sugar analysis. This work was supported by grants from the National Natural Science Foundation of China (U21A20233; 31825023), the National Key Research and Development of China (2018YFD1000800) and the Starry Night Science Fund of Zhejiang University Shanghai Institute for Advanced Study (SN-ZJU-SIAS-0011).

Competing interests

The authors declare no competing interests.

Author contributions

Y.Z. conceived the research; J.X. and Y.Z. designed the experiments; J.X. performed the research; S.L participated in the plasmid construction; L.C. participated in preparing plant materials; L.W. participated in the cell-free degradation assay; Y.D. provided suggestions for the ethylene production measurement; Z.Q. provided facilities support; J.Y. provided suggestions for the manuscript preparation; J.X. and Y.Z. wrote the manuscript with input from all co-authors.

Data availability statement

Original MS data was available at Mendeley (DOI: 10.17632/2dpjyg8bfp.1).

References

Alonso, J.M., Hirayama, T., Roman, G., Nourizadeh, S. and Ecker, J.R. (1999) EIN2, a bifunctional transducer of ethylene and stress responses in *Arabidopsis*. *Science*, **284**, 2148–2152.

Bisson, M.M.A. and Groth, G. (2011) New paradigm in ethylene signaling EIN2, the central regulator of the signaling pathway, interacts directly with the upstream receptors. *Plant Signal. Behav.* **6**, 164–166.

Bisson, M.M.A., Bleckmann, A., Allekotte, S. and Groth, G. (2009) EIN2, the central regulator of ethylene signalling, is localized at the ER membrane where it interacts with the ethylene receptor ETR1. *Biochem. J.* **424**, 1–6.

Chang, K.N., Zhong, S., Weirauch, M.T., Hon, G., Pelizzola, M., Li, H., Huang, S.S.C. *et al.* (2013) Temporal transcriptional response to ethylene gas drives growth hormone cross-regulation in Arabidopsis. *Elife*, **2**, 20.

Chao, Q.M., Rothenberg, M., Solano, R., Roman, G., Terzaghi, W. and Ecker, J.R. (1997) Activation of the ethylene gas response pathway in *Arabidopsis* by the nuclear protein ETHYLENE-INSENSITIVE3 and related proteins. *Cell*, **89**, 1133–1144.

Daviere, J.M. and Achard, P. (2016) A pivotal role of DELLAs in regulating multiple hormone signals. *Mol. Plant*, **9**, 10–20.

Deng, H., Pirrello, J., Chen, Y., Li, N., Zhu, S., Chirinos, X., Bouzayen, M. *et al.* (2018) A novel tomato F-box protein, SlEBF3, is involved in tuning ethylene signaling during plant development and climacteric fruit ripening. *Plant J.* **95**, 648–658.

Dong, Y.F., Tang, M.J., Huang, Z.L., Song, J.N., Xu, J., Ahammed, G.J., Yu, J.Q. *et al.* (2022) The miR164a-NAM3 module confers cold tolerance by inducing ethylene production in tomato. *Plant J.* **111**, 440–456.

Elliot, S.P., Schmied, R., Gabel, C.A. and Ambron, R.T. (1993) An 83 kDa *O*-GlcNAc glycoprotein is found in the axoplasm and nucleus of Aplysia neurons. *J. Neurosci.* **13**, 2424–2429.

Fantini, E. and Giuliano, G. (2016) Virus-induced gene silencing as a tool to study tomato fruit biochemistry. In *Plant Signal Transduction: Methods and Protocols*, Vol. **1363** (Botella, J.R. and Botella, M.A., eds), pp. 65–78. New York, NY: Springer New York.

Fantini, E., Falcone, G., Frusciante, S., Giliberto, L. and Giuliano, G. (2013) Dissection of tomato lycopene biosynthesis through virus-induced gene silencing. *Plant Physiol.* **163**, 986–998.

Fletcher, C.M., Coyne, M.J., Villa, O.F., Chatzidaki-Livanis, M. and Comstock, L.E. (2009) A general *O*-Glycosylation system important to the physiology of a major human intestinal symbiont. *Cell*, **137**, 321–331.

Fu, D.Q., Zhu, B.Z., Zhu, H.L., Jiang, W.B. and Luo, Y.B. (2005) Virus-induced gene silencing in tomato fruit. *Plant J.* **43**, 299–308.

Fujisawa, M., Nakano, T., Shima, Y. and Ito, Y. (2013) A large-scale identification of direct targets of the tomato MADS box transcription factor RIPENING INHIBITOR reveals the regulation of fruit ripening. *Plant Cell*, **25**, 371–386.

Gao, G., Li, C., Fan, W., Zhang, M., Li, X., Chen, W., Li, W. *et al.* (2021) Brilliant glycans and glycosylation: Seq and ye shall find. *Int. J. Biol. Macromol.* **189**, 279–291.

Giovannoni, J., Nguyen, C., Ampofo, B., Zhong, S.L. and Fei, Z.J. (2017) The epigenome and transcriptional dynamics of fruit ripening. *Annu. Rev. Plant Biol.* **68**, 61–84.

Greenboim-Wainberg, Y., Maymon, I., Borochov, R., Alvarez, J., Olszewski, N., Ori, N., Eshed, Y. *et al.* (2005) Cross talk between gibberellin and cytokinin: the *Arabidopsis* GA response inhibitor SPINDLY plays a positive role in cytokinin signaling. *Plant Cell*, **17**, 92–102.

Guo, J.E., Hu, Z.L., Li, F.F., Zhang, L.C., Yu, X.H., Tang, B.Y. and Chen, G.P. (2017) Silencing of histone deacetylase SlHDT3 delays fruit ripening and suppresses carotenoid accumulation in tomato. *Plant Sci.* **265**, 29–38.

Hamilton, A.J., Lycett, G.W. and Grierson, D. (1990) Antisense gene that inhibits synthesis of the hormone ethylene in transgenic plants. *Nature*, **346**, 284–287.

Hart, G.W., Slawson, C., Ramirez-Correa, G. and Lagerlof, O. (2011) Cross talk between *O*-GlcNAcylation and phosphorylation: roles in signaling, transcription, and chronic disease. *Annu. Rev. Biochem.* **80**, 825–858.

Hartweck, L.M., Scott, C.L. and Olszewski, N.E. (2002) Two *O*-linked *N*-acetylglucosamine transferase genes of *Arabidopsis thaliana* L. Heynh. Have

overlapping functions necessary for gamete and seed development. *Genetics*, **161**, 1279–1291.

Hartweck, L.M., Genger, R.K., Grey, W.M. and Olszewski, N.E. (2006) SECRET AGENT and SPINDLY have overlapping roles in the development of *Arabidopsis thaliana* L. Heyn. *J. Exp. Bot.* **57**, 865–875.

Holt, G.D. and Hart, G.W. (1986) The subcellular-distribution of terminal *N*-acetylglucosamine moieties-localization of a novel protein-saccharide linkage, *O*-linked GlcNAc. *J. Biol. Chem.* **261**, 8049–8057.

Huang, W., Hu, N., Xiao, Z., Qiu, Y., Yang, Y., Yang, J., Mao, X. *et al*. (2022) A molecular framework of ethylene-mediated fruit growth and ripening processes in tomato. *Plant Cell*, **34**, 3280–3300.

Johnson, P.R. and Ecker, J.R. (1998) The ethylene gas signal transduction pathway: a molecular perspective. *Annu. Rev. Genet.* **32**, 227–254.

Ju, C.L., Yoon, G.M., Shemansky, J.M., Lin, D.Y., Ying, Z.I., Chang, J.H., Garrett, W.M. *et al*. (2012) CTR1 phosphorylates the central regulator EIN2 to control ethylene hormone signaling from the ER membrane to the nucleus in Arabidopsis. *Proc. Natl. Acad. Sci. USA*, **109**, 19486–19491.

Ju, C.L., Van de Poel, B., Cooper, E.D., Thierer, J.H., Gibbons, T.R., Delwiche, C.F. and Chang, C.R. (2015) Conservation of ethylene as a plant hormone over 450 million years of evolution. *Nat. Plants*, **1**, 7.

Kamiyoshihara, Y., Tieman, D.M., Huber, D.J. and Klee, H.J. (2012) Ligand-induced alterations in the phosphorylation state of ethylene receptors in tomato fruit. *Plant Physiol.* **160**, 488–497.

Kieber, J.J., Rothenberg, M., Roman, G., Feldmann, K.A. and Ecker, J.R. (1993) *CTR1*, a negative regulator of the ethylene response pathway in *Arabidopsis*, encodes a member of the Raf family of protein-kinases. *Cell*, **72**, 427–441.

Li, W.Y., Ma, M.D., Feng, Y., Li, H.J., Wang, Y.C., Ma, Y.T., Li, M.Z. *et al*. (2015) EIN2-directed translational regulation of ethylene signaling in *Arabidopsis*. *Cell*, **163**, 670–683.

Li, Z.W., Jiang, G.X., Liu, X.C., Ding, X.C., Zhang, D.D., Wang, X.W., Zhou, Y.J. *et al*. (2020) Histone demethylase SlJMJ6 promotes fruit ripening by removing H3K27 methylation of ripening-related genes in tomato. *New Phytol.* **227**, 1138–1156.

Liu, M.C., Pirrello, J., Chervin, C., Roustan, J.P. and Bouzayen, M. (2015) Ethylene control of fruit ripening: revisiting the complex network of transcriptional regulation. *Plant Physiol.* **169**, 2380–2390.

Mao, Y.F., Zhang, H., Xu, N.F., Zhang, B.T., Gou, F. and Zhu, J.K. (2013) Application of the CRISPR-Cas system for efficient genome engineering in plants. *Mol. Plant*, **6**, 2008–2011.

Maymon, I., Greenboim-Wainberg, Y., Sagiv, S., Kieber, J.J., Moshelion, M., Olszewski, N. and Weiss, D. (2009) Cytosolic activity of SPINDLY implies the existence of a DELLA-independent gibberellin-response pathway. *Plant J.* **58**, 979–988.

Merchante, C., Brumos, J., Yun, J., Hu, Q.W., Spencer, K.R., Enriquez, P., Binder, B.M. *et al*. (2015) Gene-specific translation regulation mediated by the hormone-signaling molecule EIN2. *Cell*, **163**, 684–697.

Miernyk, J.A. and Thelen, J.J. (2008) Biochemical approaches for discovering protein-protein interactions. *Plant J.* **53**, 597–609.

Oeller, P.W., Wong, L.M., Taylor, L.P., Pike, D.A. and Theologis, A. (1991) Reversible inhibition of tomato fruit senescence by antisense RNA. *Science*, **254**, 437–439.

Ohtsubo, K. and Marth, J.D. (2006) Glycosylation in cellular mechanisms of health and disease. *Cell*, **126**, 855–867.

Olszewski, N.E., West, C.M., Sassi, S.O. and Hartweck, L.M. (2010) O-GlcNAc protein modification in plants: evolution and function. *BBA-Gen. Subjects*, **1800**, 49–56.

Qiao, H., Chang, K.N., Yazaki, J. and Ecker, J.R. (2009) Interplay between ethylene, ETP1/ETP2 F-box proteins, and degradation of EIN2 triggers ethylene responses in *Arabidopsis*. *Genes Dev.* **23**, 512–521.

Qiao, H., Shen, Z.X., Huang, S.S.C., Schmitz, R.J., Urich, M.A., Briggs, S.P. and Ecker, J.R. (2012) Processing and subcellular trafficking of ER-tethered EIN2 control response to ethylene gas. *Science*, **338**, 390–393.

Rocco, M., D'Ambrosio, C., Arena, S., Faurobert, M., Scaloni, A. and Marra, M. (2006) Proteomic analysis of tomato fruits from two ecotypes during ripening. *Proteomics*, **6**, 3781–3791.

Sarnowska, E.A., Rolicka, A.T., Bucior, E., Cwiek, P., Tohge, T., Fernie, A.R., Jikumaru, Y. *et al*. (2013) DELLA-interacting SWI3C core subunit of switch/sucrose nonfermenting chromatin remodeling complex modulates gibberellin responses and hormonal cross talk in *Arabidopsis*. *Plant Physiol.* **163**, 305–317.

Sikorskaite, S., Rajamaki, M.L., Baniulis, D., Stanys, V. and Valkonen, J.P.T. (2013) Protocol: optimised methodology for isolation of nuclei from leaves of species in the *Solanaceae* and *Rosaceae* families. *Plant Methods*, **9**, 9.

Sparkes, I.A., Runions, J., Kearns, A. and Hawes, C. (2006) Rapid, transient expression of fluorescent fusion proteins in tobacco plants and generation of stably transformed plants. *Nat. Protoc.* **1**, 2019–2025.

Steiner, E., Efroni, I., Gopalraj, M., Saathoff, K., Tseng, T.-S., Kieffer, M., Eshed, Y. *et al*. (2012) The *Arabidopsis O*-linked *N*-acetylglucosamine transferase SPINDLY interacts with class I TCPs to facilitate cytokinin responses in leaves and flowers. *Plant Cell*, **24**, 96–108.

Swain, S.M., Tseng, T.-S., Thornton, T.M., Gopalraj, M. and Olszewski, N.E. (2002) SPINDLY is a nuclear-localized repressor of gibberellin signal transduction expressed throughout the plant. *Plant Physiol.* **129**, 605–615.

Tang, D., Gallusci, P. and Lang, Z. (2020) Fruit development and epigenetic modifications. *New Phytol.* **228**, 839–844.

Waadt, R. and Kudla, J. (2008) In planta visualization of protein interactions using bimolecular fluorescence complementation (BiFC). *CSH Protocols*, **2008**, pdb.prot4995.

Wang, F., Zhu, D.M., Huang, X., Li, S., Gong, Y.N., Yao, Q.F., Fu, X.D. *et al*. (2009) Biochemical insights on degradation of *Arabidopsis* DELLA proteins gained from a cell-free assay system. *Plant Cell*, **21**, 2378–2390.

Wang, Y., Wang, W., Cai, J., Zhang, Y., Qin, G. and Tian, S. (2014) Tomato nuclear proteome reveals the involvement of specific E2 ubiquitin-conjugating enzymes in fruit ripening. *Genome Biol.* **15**, 521.

Wang, Y., He, Y.Q., Su, C., Zentella, R., Sun, T.P. and Wang, L. (2020) Nuclear localized *O*-fucosyltransferase SPY facilitates PRR5 proteolysis to fine-tune the pace of *Arabidopsis* circadian clock. *Mol. Plant*, **13**, 446–458.

Wen, X., Zhang, C.L., Ji, Y.S., Zhao, Q., He, W.R., An, F.Y., Jiang, L.W. *et al*. (2012) Activation of ethylene signaling is mediated by nuclear translocation of the cleaved EIN2 carboxyl terminus. *Cell Res.* **22**, 1613–1616.

West, C.M. and Kim, H.W. (2019) Nucleocytoplasmic *O*-glycosylation in protists. *Curr. Opin. Struct. Biol.* **56**, 204–212.

Xia, X., Dong, H., Yin, Y., Song, X., Gu, X., Sang, K., Zhou, J. *et al*. (2021) Brassinosteroid signaling integrates multiple pathways to release apical dominance in tomato. *Proc. Natl Acad. Sci. USA*, **118**, e2004384118.

Xiao, J., Xu, S.J., Li, C.H., Xu, Y.U., Xing, L.J., Niu, Y.D., Huan, Q. *et al*. (2014) *O*-GlcNAc-mediated interaction between VER2 and TaGRP2 elicits TaVRN1 mRNA accumulation during vernalization in winter wheat. *Nat. Commun.* **5**, 13.

Xing, L.J., Liu, Y., Xu, S.J., Xiao, J., Wang, B., Deng, H.W., Lu, Z. *et al*. (2018) Arabidopsis O-GlcNAc transferase SEC activates histone methyltransferase ATX1 to regulate flowering. *EMBO J.* **37**, 12.

Xu, F., Yuan, S., Zhang, D.W., Lv, X. and Lin, H.H. (2012) The role of alternative oxidase in tomato fruit ripening and its regulatory interaction with ethylene. *J. Exp. Bot.* **63**, 5705–5716.

Xu, S.L., Chalkley, R.J., Maynard, J.C., Wang, W., Ni, W., Jiang, X., Shin, K. *et al*. (2017) Proteomic analysis reveals *O*-GlcNAc modification on proteins with key regulatory functions in *Arabidopsis*. *Proc. Natl. Acad. Sci. USA*, **114**, 1536–1543.

Zachara, N.E. and Hart, G.W. (2006) Cell signaling, the essential role of *O*-GlcNAc! *BBA-Mol. Cell Biol. Lipids*, **1761**, 599–617.

Zentella, R., Hu, J., Hsieh, W.-P., Matsumoto, P.A., Dawdy, A., Barnhill, B., Oldenhof, H. *et al*. (2016) *O*-GlcNAcylation of master growth repressor DELLA by SECRET AGENT modulates multiple signaling pathways in *Arabidopsis*. *Genes Dev.* **30**, 164–176.

Zentella, R., Sui, N., Barnhill, B., Hsieh, W.P., Hu, J.H., Shabanowitz, J., Boyce, M. *et al*. (2017) The Arabidopsis *O*-fucosyltransferase SPINDLY activates nuclear growth repressor DELLA. *Nat. Chem. Biol.* **13**, 479–485.

Zhang, F., Wang, L., Qi, B., Zhao, B., Ko, E.E., Riggan, N.D., Chin, K. *et al*. (2017) EIN2 mediates direct regulation of histone acetylation in the ethylene response. *Proc. Natl Acad. Sci. USA*, **114**, 10274–10279.

Supporting information

Additional supporting information may be found online in the Supporting Information section at the end of the article.

Figure S1 Generation of tomato *slspy* mutants and *SlSPY* overexpressing plants.
Figure S2 Relative transcript levels of ripening-related genes in *slspy* mutants, *35Spro: SlSPY*-HA and WT fruits at different ripening stages were determined by qRT-PCR.
Figure S3 Ethylene production in *slspy* mutants, *35Spro: SlSPY*-HA and WT fruits.
Figure S4 Physical interactions between SlSPY or SlSEC1 and SlEIN2.
Figure S5 Mapping the site of *O*-glycosylation on SlEIN2 using mass spectrometry.
Figure S6 Relative transcript levels of *SlEIN2* in *slspy* mutants, *35Spro: SlSPY*-HA and WT plants.
Figure S7 SlSPY regulates nuclear accumulation of SlEIN2.
Figure S8 SlSPY is involved in ethylene signalling.
Figure S9 Ethylene-related phenotypes in *slspy* mutants, *35Spro: SlSPY*-HA and WT plants.
Movie S1 A 3D image showing that SlEIN2 interacts with SlSPY is present in cytoplasmic foci.
Table S1 Off-target detection in *slspy* mutants in T0 generation.
Table S2 The identified proteins that interact with SlSPY in the Y-2-H screen.
Table S3 PCR primer sequences used for constructing of mutant line vectors.
Table S4 Primer sequences used for constructing eukaryotic expression vectors.
Table S5 Primer sequences used for qRT-PCR analysis.
Table S6 Primer sequences used for constructing prokaryotic expression vectors.
Table S7 Primer sequences used for the yeast two-hybrid (Y-2-H) assays.

